Stratigraphy of the Northeast Syrtis Major Mars 2020 Landing Site and the Ejecta of Jezero Crater, Mars

Michael S. Bramble[1], John F. Mustard[1], Caleb I. Fassett[2], and Timothy A. Goudge[3]

1. Department of Earth, Environmental, and Planetary Sciences, Brown University, 2. NASA Marshall Space Flight Center, 3. Jackson School of Geosciences, The University of Texas at Austin

The five-second spiel:

The NE Syrtis Mars 2020 candidate landing site is located in a region that would have been affected by the emplacement of Jezero's continuous ejecta. We search for and find no apparent evidence of remnant ejecta, and use morphology, topography, and stratigraphy to gauge the amount of erosion that occurred. Erosion is apparent prior to the circum-Isidis olivine-rich unit's deposition, and large linear features may be related to both regional stress and aeolian processes.

Introduction:

The NE Syrtis landing ellipse [1,2] is located at approximately one crater radius beyond the rim of Jezero crater (**Figure 1**), a region likely near or within the area that was affected by emplacement of Jezero's continuous ejecta. Therefore, excavated material 10s to ~100 m thick may have been locally deposited [3–5]. Because of Jezero's Noachian age, however, its ejecta may have been entirely removed from the stratigraphic record at NE Syrtis via erosion.Whether remnants of Jezero's ejecta persist has significant implications for the local erosional history, the stratigraphy at the landing site, and the origin of the materials now exposed at the surface.

Of particular interest are the Large Linear Features (LLF) of [2], light-toned linear structures 10s to 100s of meters wide and 1000s of meters long that qualitatively appear radial to Jezero (**Figure 2**). We focus on the morphology, topography, and stratigraphy of the LLF and basement unit of [2] to search for evidence of Jezero ejecta and clues to the landscape evolution of the region.

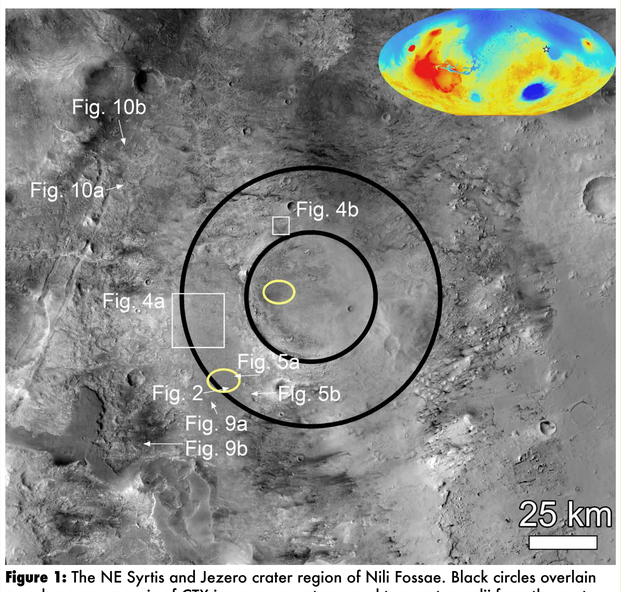

Figure 1: The NE Syrtis and Jezero crater region of Nili Fossae. Black circles overlain on a basemap mosaic of CTX imagery are at one and two crater radii from the center of Jezero crater. The candidate landing ellipses for NE Syrtis and Jezero crater are shown in yellow. The NE Syrtis ellipse is one crater radius from the rim of Jezero crater. The spatial locations of subsequent figures are shown. The top-right inset shows the location of the NE Syrtis region (white star) on the global MOLA topographic map.

Methods:

The orientations of the LLF were surveyed within a square six Jezero crater radii across and centered on Jezero using Context Camera (CTX) [6] mosaics. LLF were mapped if: (1) they were identified as LLF in [2], or (2) if a feature >500 m matched LLF characteristics.

Radial profiles were taken using a Mars Orbiter Laser Altimeter (MOLA) [7] elevation map and digital elevation models (DEMs) produced using CTX stereo pairs and the NASA Ames Stereo Pipeline [8–10].

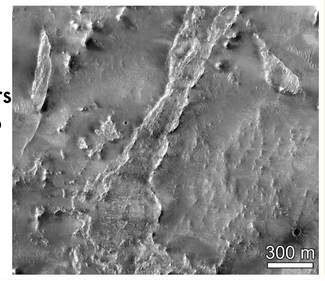

Figure 2: Example of the Large Linear Features. Image is a subframe from a mosaic of HiRISE imagery NE Syrtis.

Orientations of the Large Linear Features:

The LLF are morphological features of the regional olivine-rich unit (**Figure 2**), and are hypothesized to be mineralized fracture zones, material infilling troughs, and/or breccia or igneous dykes [2,11].

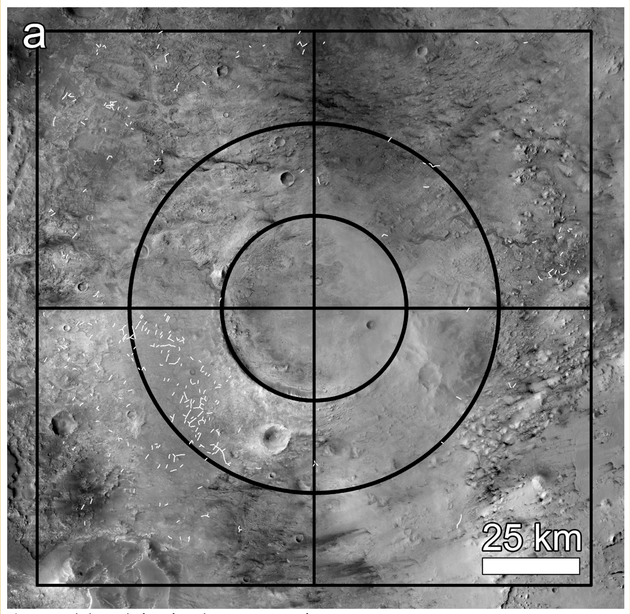

Figure 3: (a) LLF (white lines) were mapped in a square 6 crater radii centered on Jezero crater. Mapping was performed at 1:10,000 scale. (b) The LLF in this region (black) show a preferred orientation to the NE. The red arrow shows the mean of the orientation frequency distribution the large Nili Fossae troughs [12]. Note the standard deviation on the red arrow is 35.2° and is based on a N of 17 [12].

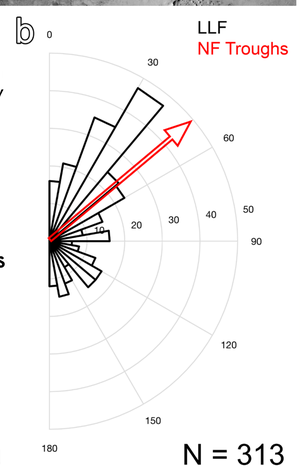

The orientation distribution of LLFs show a preference to the NE, and the signal appears regional, not related to radial fabric from Jezero crater (**Figure 3**). The NE orientation distribution matches closely with that of the Nili Fossae troughs [12], alluding to a relationship between the LLF and fracturing from regional stresses.

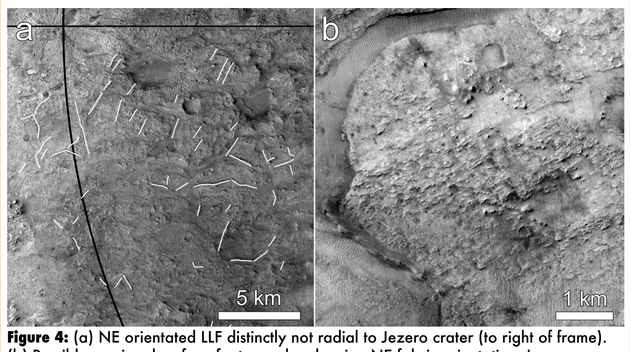

Figure 4: (a) NE orientated LLF distinctly not radial to Jezero crater (to right of frame). (b) Possible erosional surface features also showing NE fabric orientation. Images are subframes of a CTX mosaic covering Jezero crater shown in Figure 1.

Aeolian erosion may be preferentially favoring LLF formation in the observed orientation from a dominant wind direction (**Figure 4**). Outstanding issues remain, such as the angular nature seen at many LLF intersections (**Figure 5**).

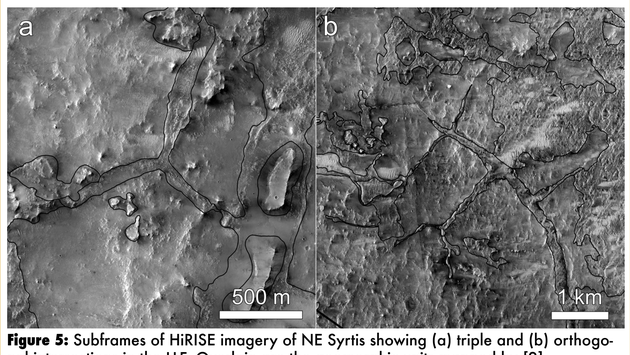

Figure 5: Subframes of HiRISE imagery of NE Syrtis showing (a) triple and (b) orthogonal intersections in the LLF. Overlain are the geomorphic units mapped by [2].

Angular intersections are not suggestive of aeolian processes, but rather may support the infilling of a fractured basement by the olivine-rich unit.

Topography:

The topography of NE Syrtis radial to Jezero crater was investigated to aid in constraining the geological history of the region.

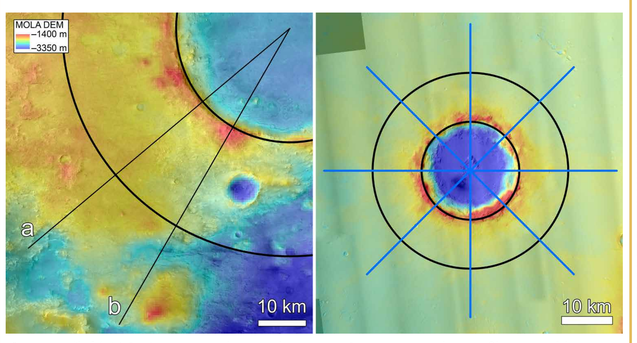

Figure 6: (left) MOLA topography overlain on a CTX mosaic. The profiles a and b corresponding to the below plots are shown. (right) Radial profiles of 8 cardinal directions of an unnamed crater in Isidis Planitia (10 °N, 94 °E). MOLA topography overlain on a mosaic of CTX imagery.

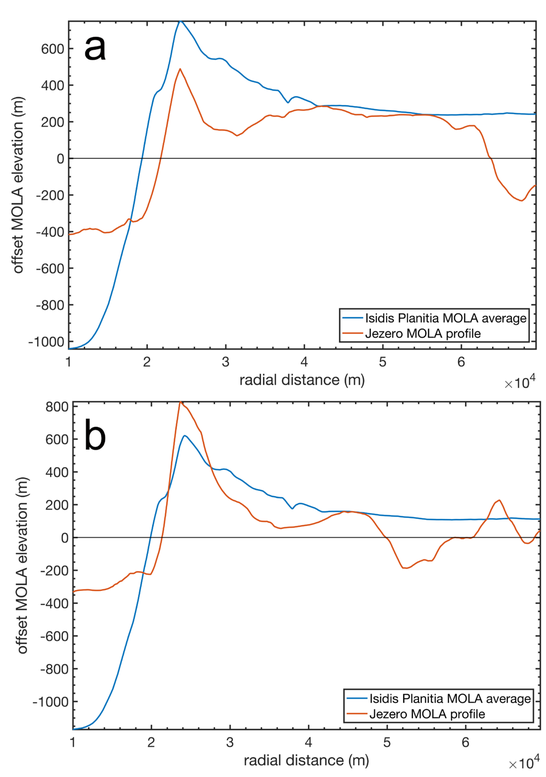

Figure 7: (a) MOLA radial profile through NE Syrtis shown in comparison to the averaged Isidis Planitia crater profile (see Figure 6). Matching high points at NE Syrtis shows the rim would have been lowered ~250 m if NE Syrtis were the immediate post-Jezero surface. (b) As in (a) but showing Jezero's rim high-standing by ~200 m if NE Syrtis were proximal to the original post-Jezero topography.

Matching the Isidis Planitia crater profile to the plains at NE Syrtis shows the eroded rim of Jezero is not a useful reference point (**Figure 7**). Comparing NE Syrtis radial profiles with the Isidis Planitia crater show that the high-points of Jezero rim could suggest ~200 m of landscape lowering at NE Syrtis. These observations are complicated by the regional slope to the south, which may explain much of the radial topographic variability.

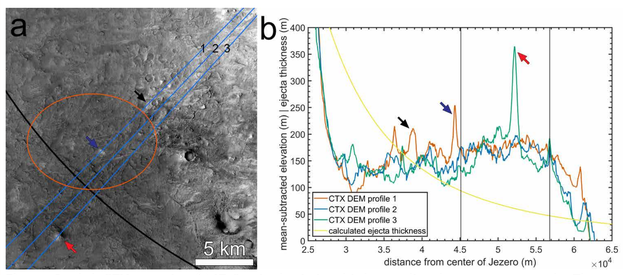

Figure 8: (a) CTX mosaic of NE Syrtis depicting high-standing basement mounds. Three numbered CTX radial profiles are shown with arrows depicting notable mounds seen in (b). (b) Mean-subtracted profiles derived from a mosaic of CTX DEMs depicting high-standing basement mounds. A calculated ejecta thickness using a radial power law [4] and the total thickness of MC9 from [5] is plotted for comparison with the basement mound heights. Vertical black lines show the near and far points of the ellipse.

Near the ellipse, mounds 50–100 m height are observed, and, if taken to be the proximal to original ejecta surface, they could suggest erosion on the order of expected ejecta (~50 m) (**Figure 8**).

Stratigraphy:

Stratigraphic relationships offer a valuable way to constrain the basement beneath the olivine-rich unit. Here we compare illustrative examples of the lower contact of the olivine-rich unit at NE Syrtis to the greater Isidis region.

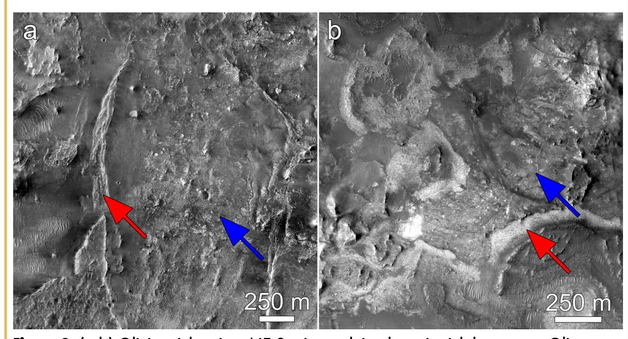

Figure 9: (a,b) Olivine-rich unit at NE Syrtis overlying breccia-rich basement. Olivine-rich outcrops are shown with the red arrows, and breccia outcrops with blue. Figures are subframes of HiRISE imagery, and image locations are shown in Figure 1.

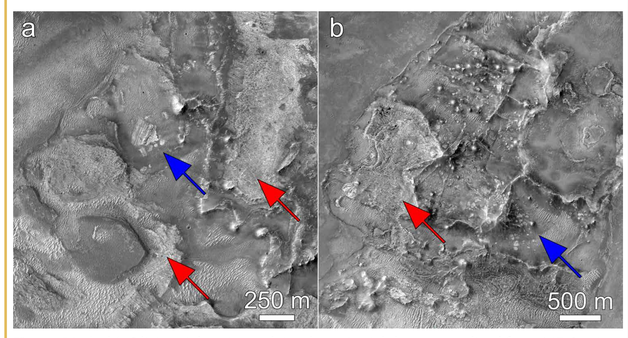

Figure 10: (a,b) Olivine-rich unit overlying breccia-rich basement distal from NE Syrtis. Olivine-rich outcrops are shown with the red arrows, and breccia outcrops with blue. Figures are subframes of HiRISE imagery, and image locations are shown in Figure 1.

At contacts between the olivine-rich unit and the down-section basement, megabreccia abutting the olivine-rich unit at NE Syrtis is observed (**Figure 9**). Similar relationships are seen at throughout Nili Fossae (**Figure 10**). No variation in this stratigraphic package is observed throughout the Nili Fossae region.

Conclusions:

- LLF at NE Syrtis are radial to Jezero crater, but this orientation distribution is a regional signal that is perhaps best explained by regional aeolian erosion and infilling of fractures formed from regional stresses related to the Isidis basin and the Nili Fossae.
- Matching radial topographic profiles of NE Syrtis to a younger crater of Jezero's size may suggest the landscape has been lowered >200 m by erosion.
- The basement mounds at NE Syrtis show that erosion has removed material equal to or greater than estimated ejecta thicknesses prior to the olivine-rich unit deposition.

An updated geological history of NE Syrtis unifying these observations would include, in order:

1. Formation of the Isidis basin
2. Fracturing of the regional basement from impact events or regional stresses, possibly related to the Nili Fossae
3. The formation of Jezero crater
4. Deposition recorded inside Jezero crater
5. Regional erosion exposing NE orientated troughs and fractured bedrock
6. Deposition of the circum-Isidis olivine-rich unit
7. Groundwater flow following the fractures and indurating them, making them less susceptible to erosion
8. Aeolian erosion exposing the in-filled fractures and forming landforms following the prevailing wind pattern

Acknowledgments: We utilized data products produced by Jay Dickson and the Bruce Murray Laboratory for Planetary Visualization.

References: [1] Ehlmann B. L. and Mustard J. F. (2012) *GRL*, 39, L11202. [2] Bramble M. S. et al. (2017) *Icarus*, 293, 66–93. [3] Melosh H. J. (2011) *Cambridge University Press* (9780511977848). [4] McGetchin T. R. et al. (1973) *EPSL*, 20, 226–236. [5] Sturm S. et al. (2016) *JGR*, 121, 1026–1053. [6] Malin M. C. et al. (2007) *JGR*, 112, E05S04. [7] Smith D. E. et al. (2001) *JGR*, 106, 23689–23722. [8] Broxton M. J. and Edwards L. J. (2008) *LPS XXXIX*, Abstract #2419. [9] Moratto Z. M. et al. (2010) *LPS XLI*, Abstract #2364. [10] Shean, D. E. et al. (2016) *ISPRS J. Photogramm. Re-mote Sens.*, 116, 101–117. [11] Thomas et al. (2017) *GRL*, 44, 6579–6588. [12] Saper L. and Mustard J. F. (2013) *GRL*, 40, 245–249.